Supplementary data for article:

Grozdanovic, M. M.; Drakulić, B. J.; Gavrović-Jankulović, M. Conformational Mobility of Active and E-64-Inhibited Actinidin. *Biochimica et Biophysica Acta: General Subjects* **2013**, *1830* (10), 4790–4799. https://doi.org/10.1016/j.bbagen.2013.06.015

Active and inhibited actinidin reveal remarkably different conformational mobility

*Milica Grozdanovic, Branko J. Drakulić, Marija Gavrovic-Jankulovic**

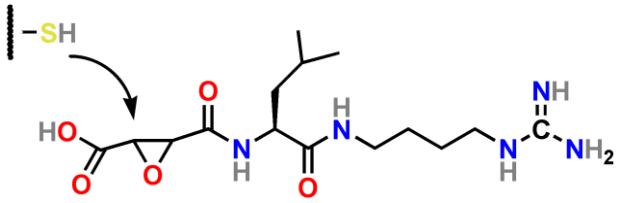

Figure S1. Structure of E64.

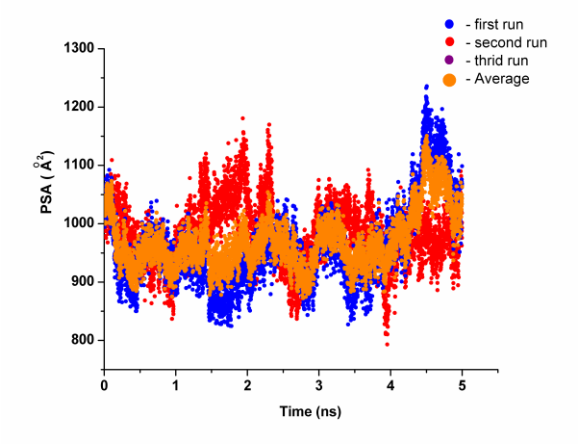

a)

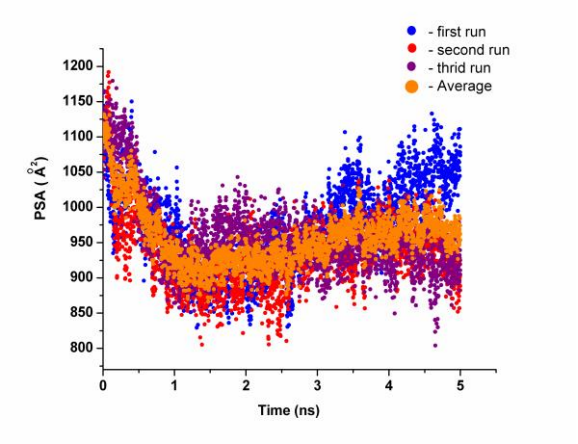

b)

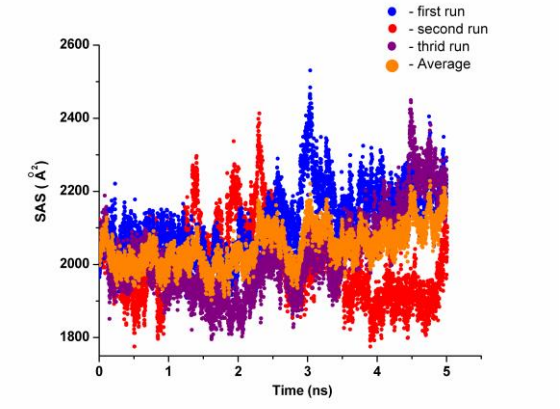

c)

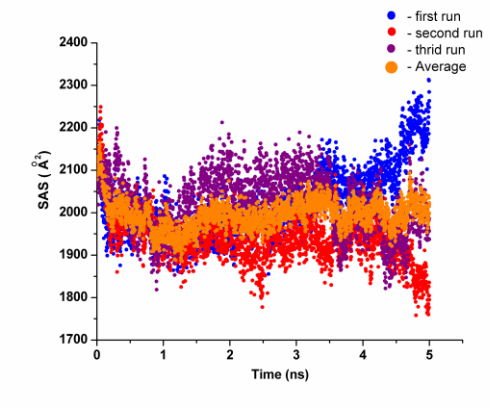

d)

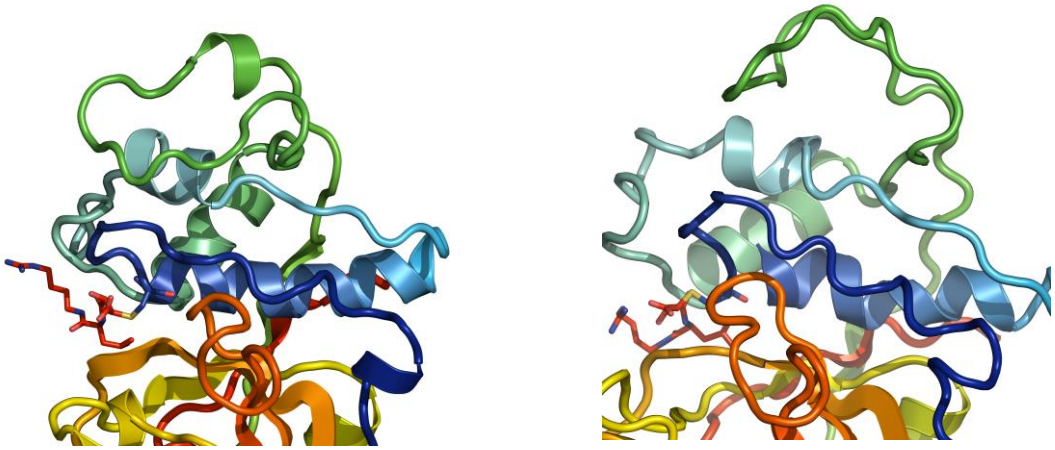

e) f)

Figure S2. Polar surface area (PSA) of a) IACT, and b) UACT. Solvent assessable area of c) IACT, and d) UACT. Conformation of the upper loop of IACT and the E64 e) after equilibration, and f) after 5 ns of MD simulation.

Figure S3. Sequences 18-28 and 90-97 of IACT (yellow) superimposed on the structure of UACT (red).

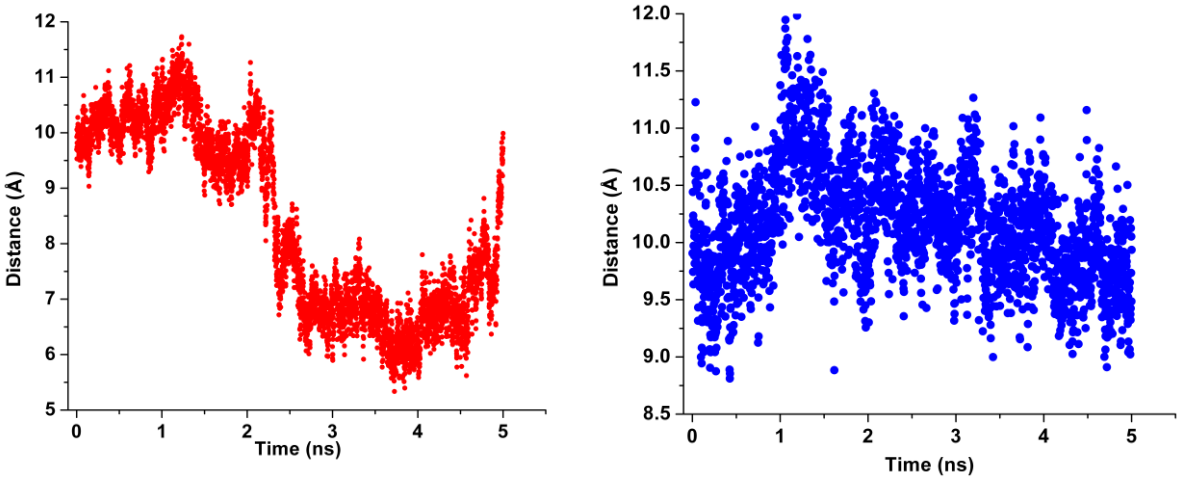

a) b)

Figure S4. Distance between centroids of TYR's 89 and 91 during 5 ns of MD simulation. a) IACT, b) UACT.

Figure S5. Overall displacement of sequence ASP15-SER47 during MD simulation of IACT. Red – whole protein after equilibration, blue – sequence after 5 ns.

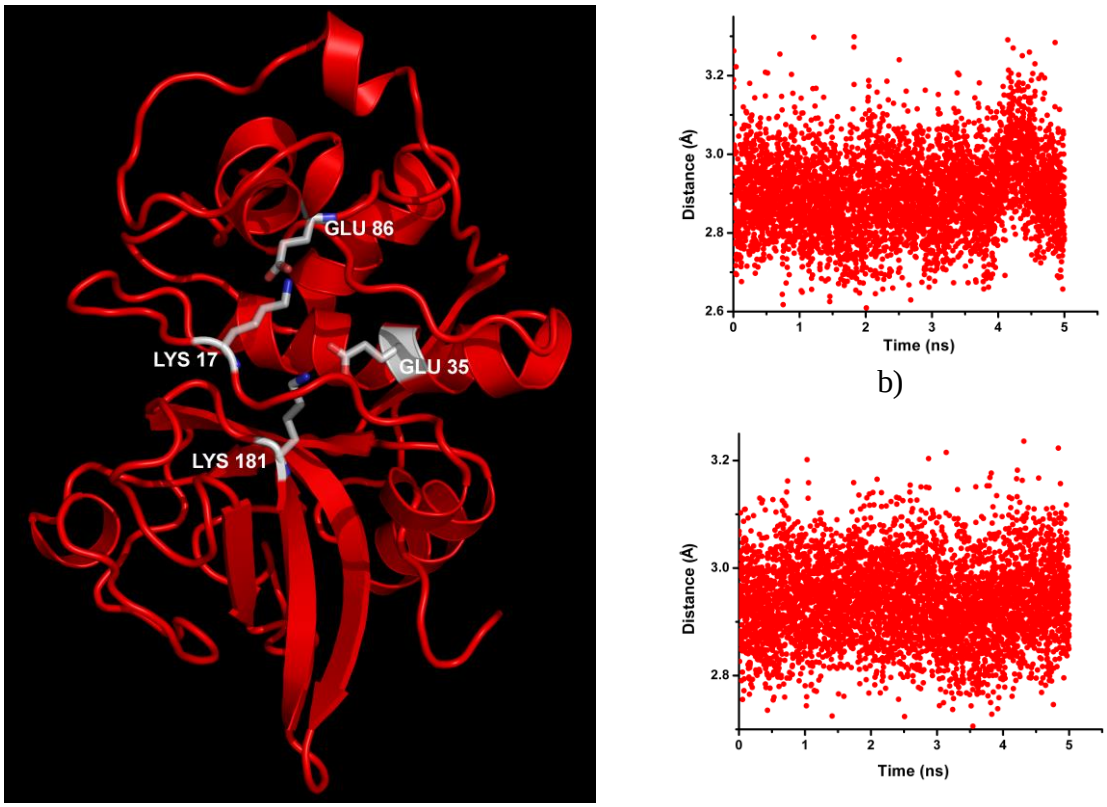

a) b) c)

Figure S6. Stabilization of actinidin subunits by salt bridges. a) Salt bridges LYS17-GLU86 and LYS181-GLU35. b) Distance LYS17 NZ – GLU86 CD during 5 ns. c) Distance LYS181 NZ – GLU35 CD during 5 ns.
Calculated from IACT.

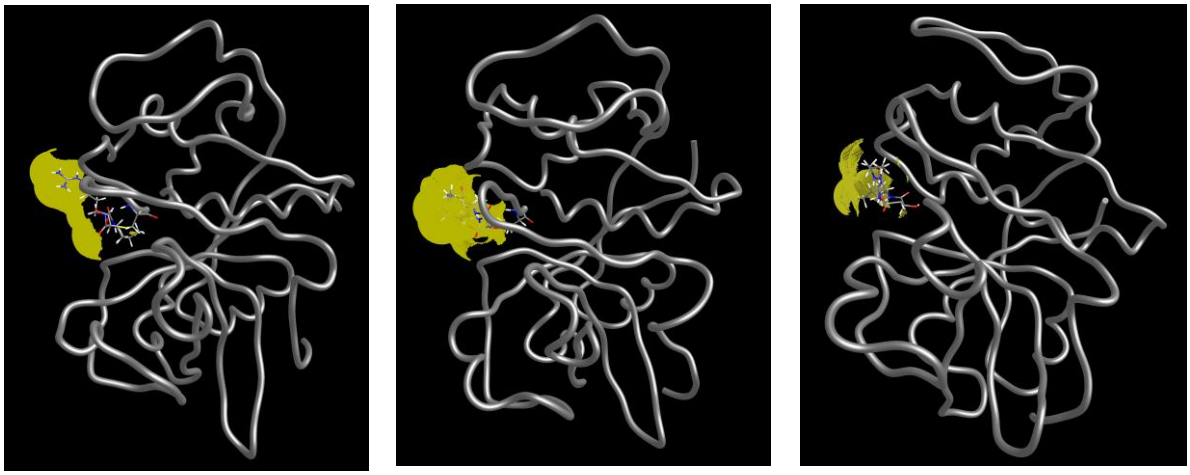

a) b) c)

Figure S7. Solvent assessable surface area of the E-64 in different conformations. See Table 1 in the main text: a) Conformation 1, b) Conformation 2, c) Conformation 4.

Table S1. Carboxylate to guanidino distance* and hydrogen bonds of guanidino moiety found in crystal structures of the E-64 co-crystallized with cysteine proteases.

PDB code	Distance	Enzyme	Specie	H-bonds of guanidino part		
				Crystal water	Residue	Reference
4D8E	13.21	SpeB	*Streptococcus pyogenes*	641, 943	/	ref 48
3IOQ	12.29	CMS1MS2	*Carica candamarcensis*	308	/	S1
3H7D	14.02	Cathepsin K	Human	222, 302, 347	Glu59	S2
2UZJ	12.92	MSPEB	*Streptococcus pyogenes*	/	/	S3
3C9E	13.25	Cathepsin K	Human	805	Glu59	S4
3BPF	11.81	Falcipain-2	*Plasmodium falciparum*	/	Asn81	S5
3BCN	11.17	Ervatamin A	*Tabernaemontana divaricata*	/	/	S6
2PRE	13.75	Ervatamin C	- II -	387	/	S6
2BDZ	10.85	Mexicain	*Jacaratia mexicana*	/	Asp64, Gln92	S7
1TLO	12.34	Calpain	Rat	/	Glu212	S8
1QX6	9.85	Sortase B	*Staphylococcus aureus*	/	/	S9
1CV8	12.64	Cystein protinase	*Staphylococcus aureus*	/	Glu69	S10
1MEG	14.01	Caricain	*Carica papaya*	/	/	S11
1ATK	12.96	Cathepsin K	Human	/	Glu59, Asp61	S12
1AEC	12.53	Actinidin	*Actinidia chinensis*	272, 403	/	ref 13

***Measured as -COO to $(NH_2)_2$CNH- distance.**

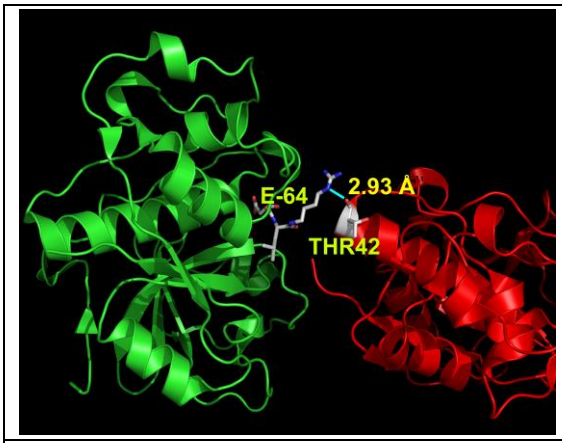

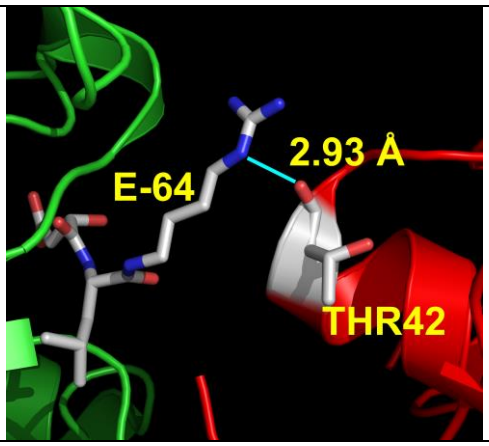

a) **b)**

PDB entry 3IOQ

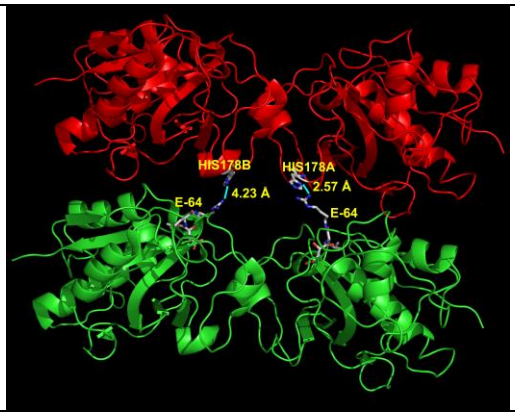

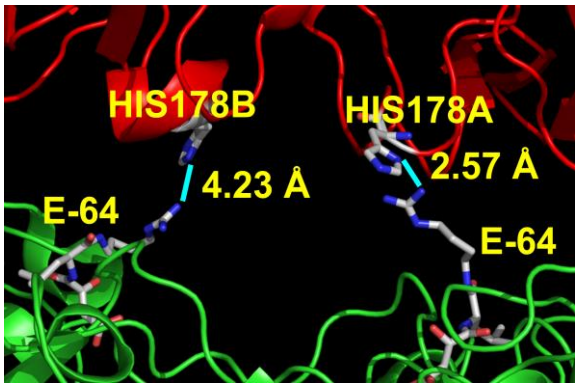

a) **b)**

PDB entry 3BCN

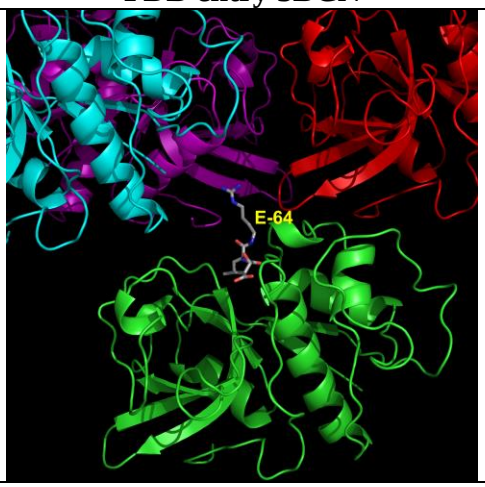

PDB entry 1MEG

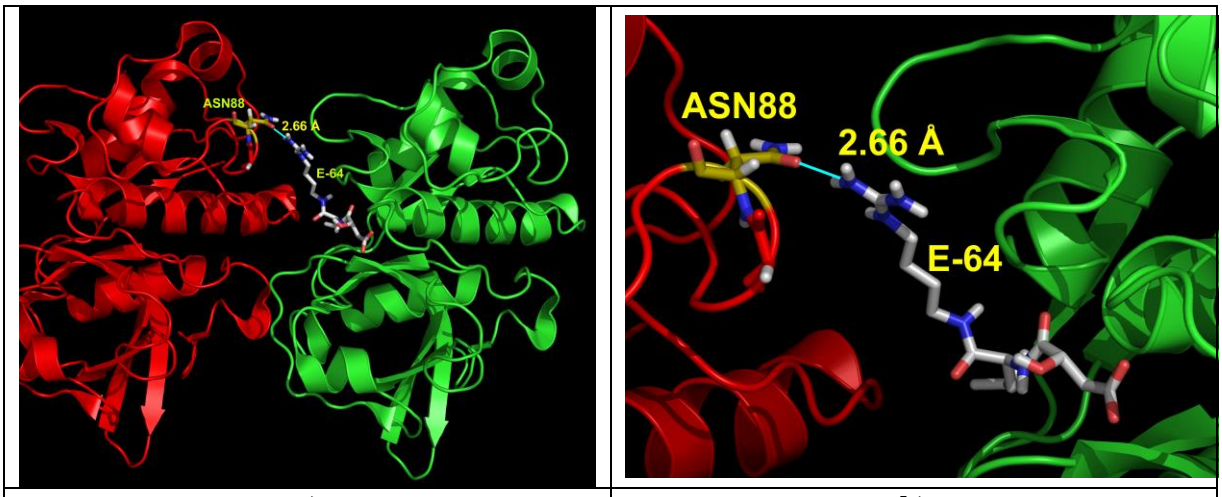

a)	b)
PDB entry 1AEC	

Figure S8. Intramolecular contacts of E-64 found with neighboring unit of crystal packing of plant cysteine proteases listed in Table S1. a) Depiction of whole units. b) Enlarged detail. For PDB entry 2PRE crystal packing did not allow such analysis.

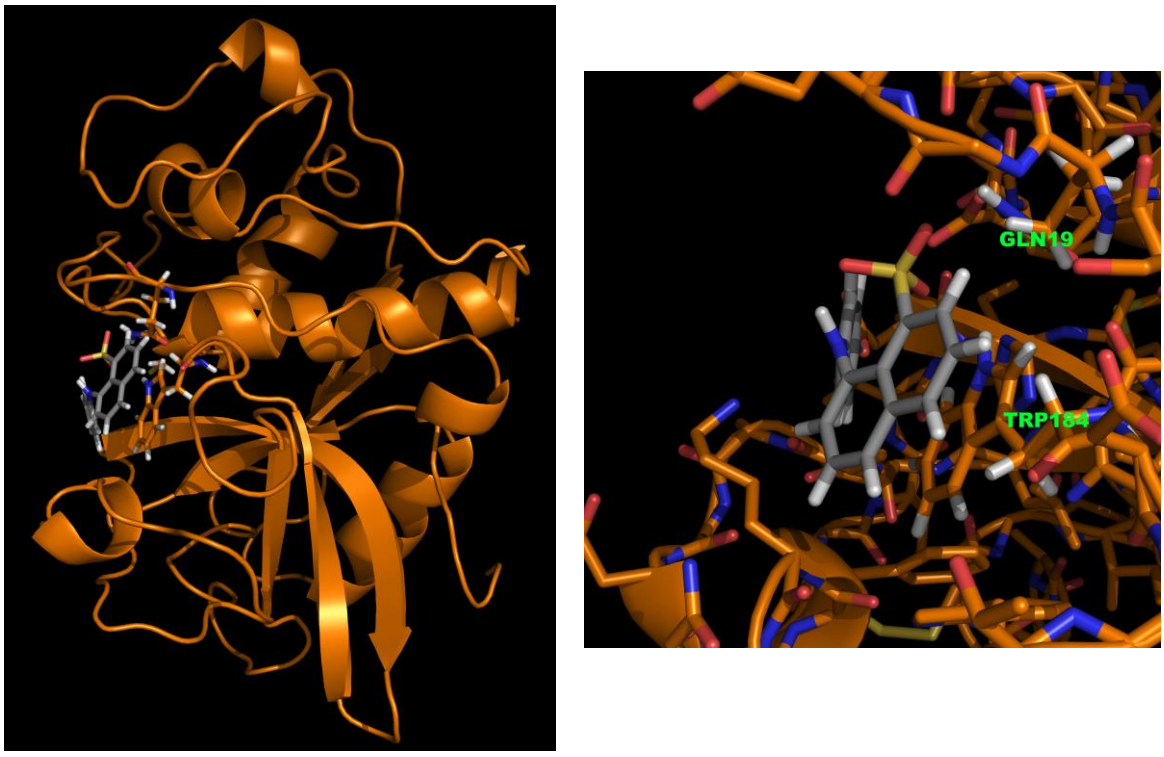

a) b)

Figure S9. ANS docked in equilibrated structure of IACT. a) Depiction of the whole protein. b) Enlarged detail.

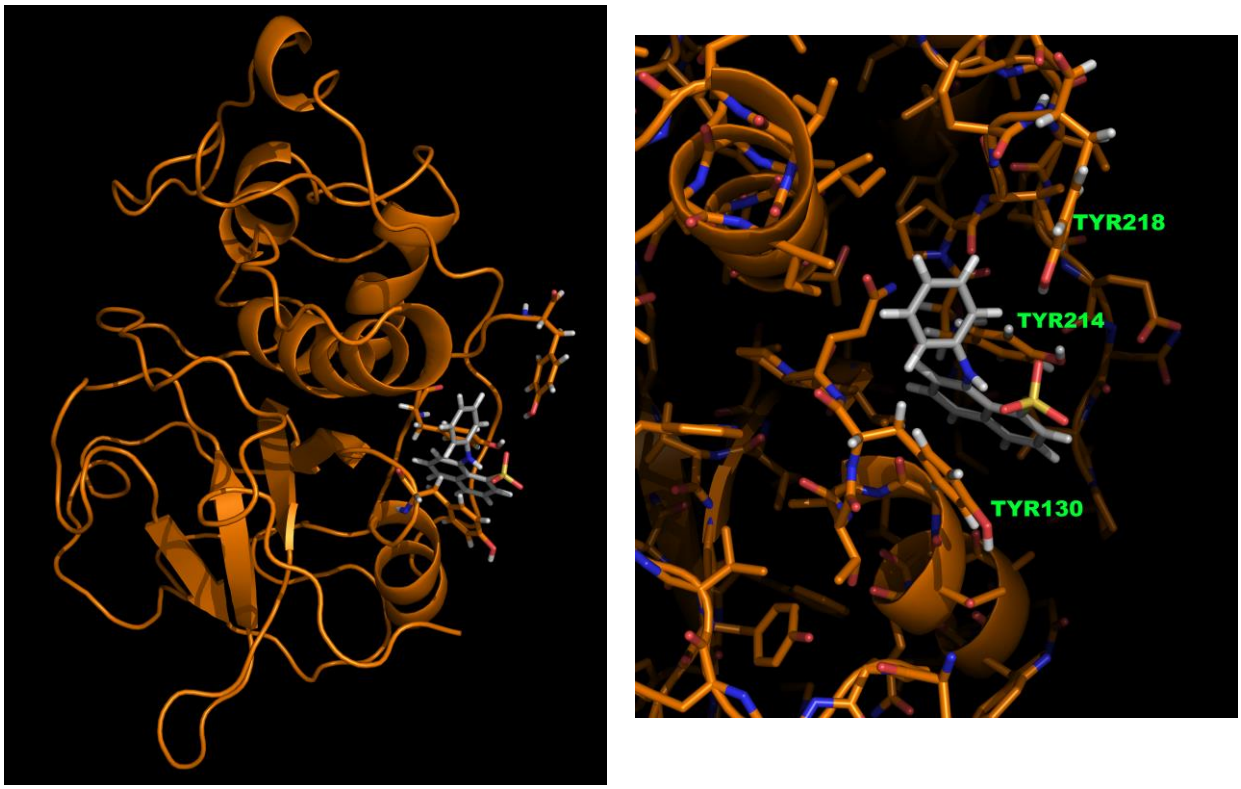

a) b)

Figure S10. ANS docked in equilibrated structure of UACT. a) Depiction of the whole protein. b) Enlarged detail.

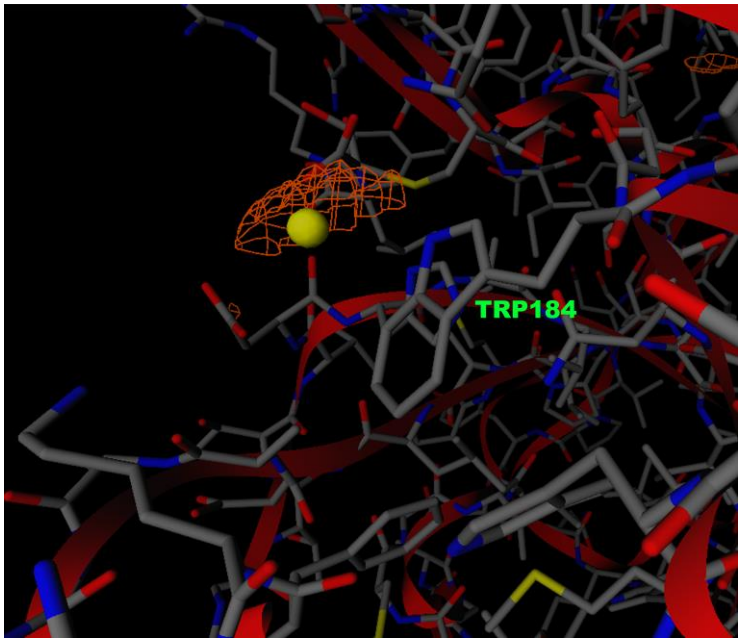

Figure S11. Global minimum (yellow sphere) of GRID DRY molecular interaction field on equilibrated IACT.

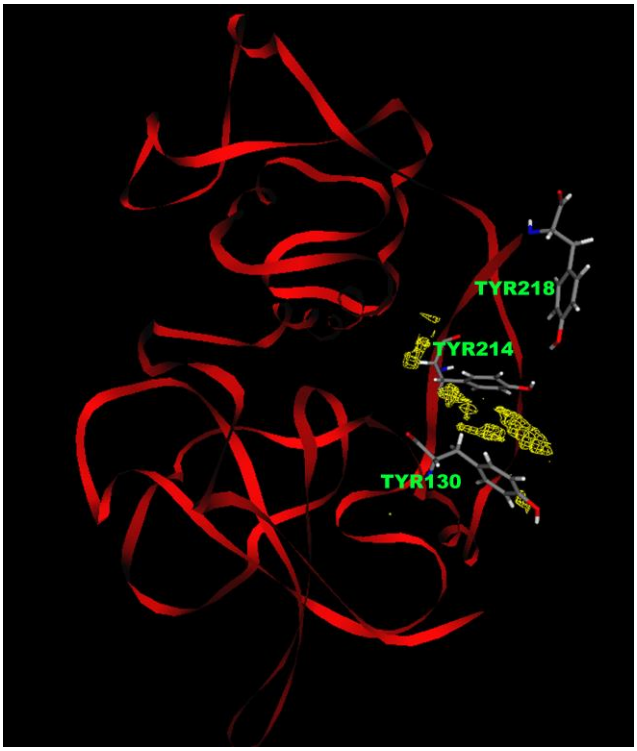

Figure S12. Volume of GRID DRY molecular interaction field depicted in the cleft lined with TYR130, TYR214 and TYR218 of equilibrated UACT.

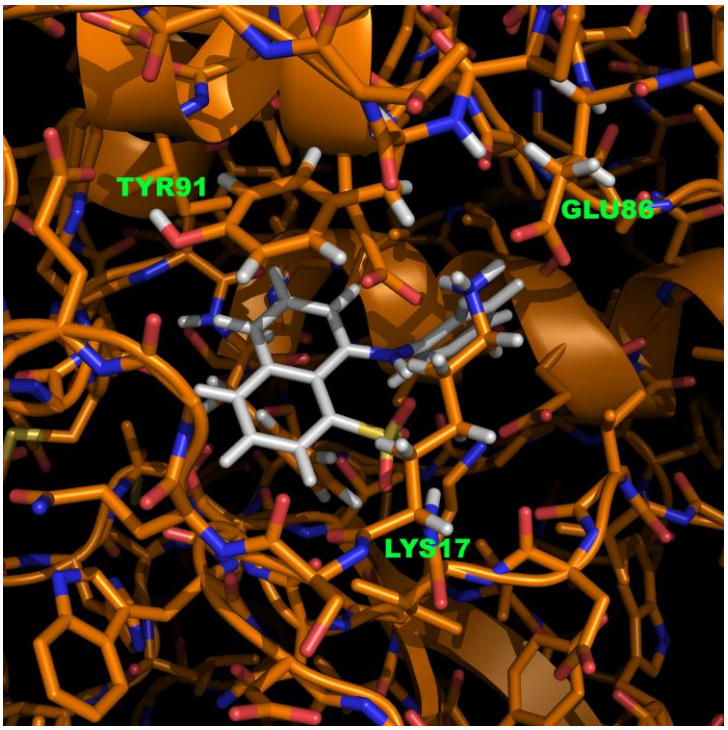

Figure S13. ANS docked structure of IACT, obtained after 5 ns of MD simulation.

Table S2. Best ranked poses in the docking solutions of the ANS and modeled actinidin, as obtained by Chemgauss4 scoring function in FRED.

Components of the score	IACT eq.[1]	UACT eq.	IACT 5 ns[#]	UACT 5 ns
Overall	–8.45	–7.14	–11.39	–7.97
Steric	–11.17	–9.69	–16.20	–10.07
Protein Desolvation	2.95	1.78	3.55	1.64
Ligand Desolvation	1.63	1.33	2.75	1.73
H-bonding	–1.86	–0.56	–1.49	–1.26

1 eq. – docked in equilibrated structure of the protein, as obtained by MD simulation; [#] 5 ns – docked in conformation of protein after 5 ns of MD simulation.

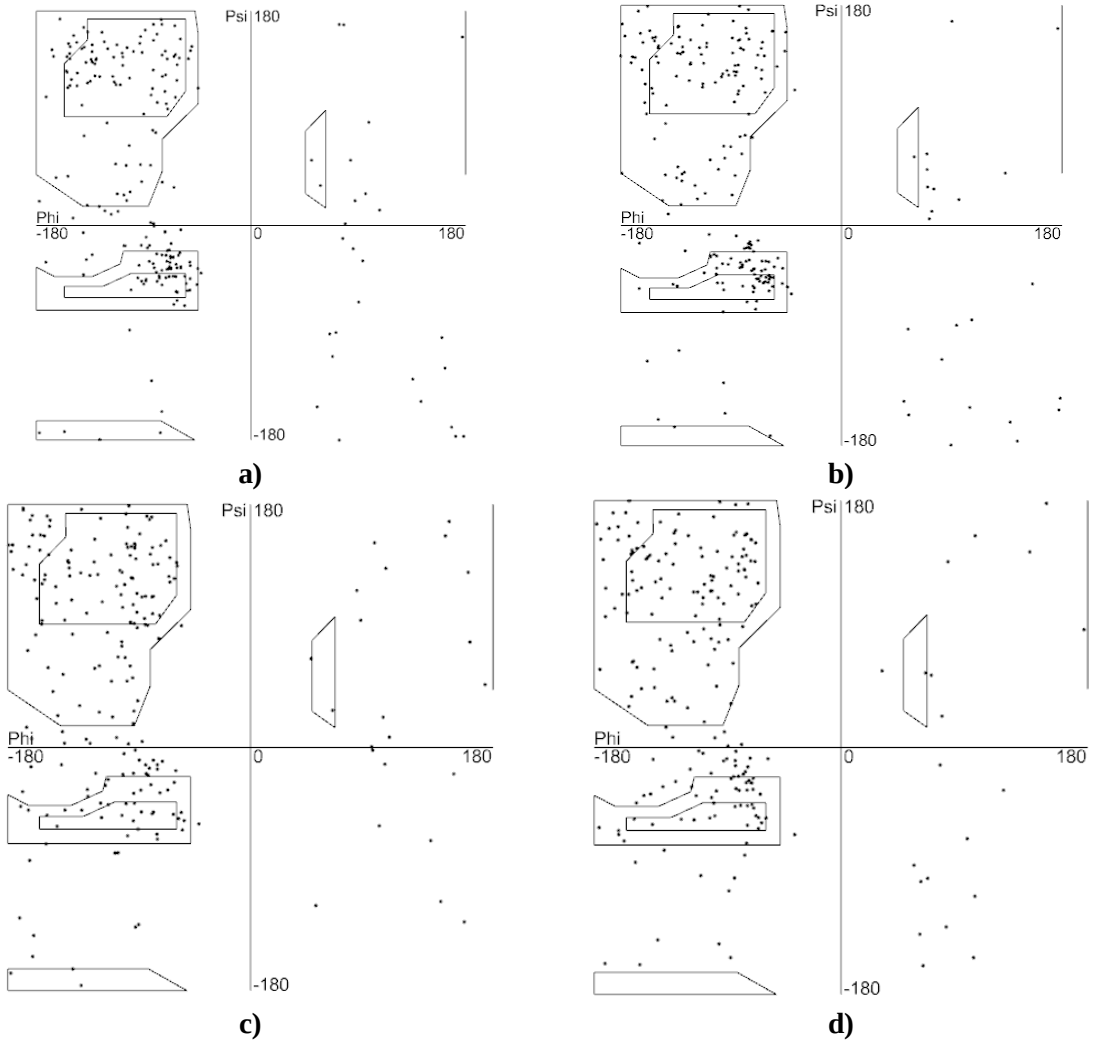

Figure S14. Ramachandran plots of IACT and UACT, after equilibration (**a** and **b**), and after the 5 ns of simulations (**c** and **d**).

Supplementary references

S1. M.T.R. Gomes, R.D. Teixeira, C.E. Salas, R.A.P. Nagem, Crystal structure of the Carica candamarcensis cysteine protease CMS1MS2 in complex with E-64 (2011), DOI:10.2210/pdb3ioq/pdb

S2. M.M. Cherney, M. Kienetz, D. Bromme, M.N.G. James, The crystal structure of the cathepsin K Variant M5 in complex with chondroitin-4-sulfate (2011), DOI:10.2210/pdb3h7d/pdb

S3. J.G. Olsen, R. Dagil, L.M. Niclasen, O.E. Soerensen, B.B. Kragelund, Structure of the mature Streptococcal cysteine protease exotoxin mSpeB in its active dimeric form, J.Mol.Biol. 393 (2009) 693-703.

S4. Z. Li, M. Kienetz, M.M. Cherney, M.N. James, D. Bromme, The crystal and molecular structures of a cathepsin K:chondroitin sulfate complex, J.Mol.Biol. 383 (2008) 78-91.

S5. I.D. Kerr, J.H. Lee, K.C. Pandey, A. Harrison, M. Sajid, P.J. Rosenthal, L.S. Brinen, Structures of falcipain-2 and falcipain-3 bound to small molecule inhibitors: implications for substrate specificity, J.Med.Chem. 52 (2009) 852-857.

S6. R. Ghosh, S. Chakraborty, C. Chakrabarti, J.K. Dattagupta, S. Biswas, Structural insights into the substrate specificity and activity of ervatamins, the papain-like cysteine proteases from a tropical plant, *Ervatamia coronaria*, Febs J. 275 (2008) 421-434.

S7. J.A. Gavira, M.C. Oliver-Salvador, L.A. Gonzalez-Ramirez, M. Soriano-Garcia, J.M. Garcia-Ruiz Crystallographic structure of Mexicain from Jacaratia mexicana (2011), DOI:10.2210/pdb2bdz/pdb

S8. T. Moldoveanu, R.L. Campbell, D. Cuerrier, P.L. Davies, Crystal structures of calpain-E64 and -leupeptin inhibitor complexes reveal mobile loops gating the active site, J.Mol.Biol. 343 (2004) 1313-1326.

S9. Y. Zong, S.K. Mazmanian, O. Schneewind, S.V. Narayana, The structure of sortase B, a cysteine transpeptidase that tethers surface protein to the *Staphylococcus aureus* cell wall, Structure 12 (2004) 105-112.

S10. B. Hofmann, D. Schomburg, H.J. Hecht, Crystal Structure of a Thiol Proteinase from *Staphylococcus Aureus* V-8 in the E-64 Inhibitor Complex, Acta Crystallogr. Sect.A 49 (1993) 102.

S11. N.A. Katerelos, M.A. Taylor, M. Scott, P.W. Goodenough, R.W. Pickersgill, Crystal structure of a caricain D158E mutant in complex with E-64, FEBS Lett. 392 (1996) 35-39.

S12. B. Zhao, C.A. Janson, B.Y. Amegadzie, K. D'Alessio, C. Griffin, C.R. Hanning, C. Jones, J. Kurdyla, M. McQueney, X. Qiu, W.W. Smith, S.S. Abdel-Meguid, Crystal structure of human osteoclast cathepsin K complex with E-64, Nat.Struct.Biol. 4 (1997) 109-111.